Finite element analysis of mechanical behavior of concrete-filled square steel tube short columns with inner I-shaped CFRP profiles subjected to bi-axial eccentric load

G. Li*, Z. Zhan, Z. Yang, Y. Yang

School Of Civil Engineering, Shenyang Jianzhu University, China
*corresponding author, e-mail address: liguochang0604@sina.com

Abstract

The concrete-filed square steel tube with inner I-shaped CFRP profiles short columns under bi-axial eccentric load were investigated by the finite element analysis software ABAQUS. The working mechanism of the composite columns which is under bi-axial eccentric load are investigated by using the stress distribution diagram of steel tube concrete and the I-shaped CFRP profiles. In this paper, the main parameters; eccentric ratio, steel ratio, steel yield strength, concrete compressive strength and CFRP distribution rate of the specimens were investigated to know the mechanical behavior of them. The interaction between the steel tube and the concrete interface at different characteristic points of the composite columns were analyzed. The results showed that the ultimate bearing capacity of the concrete-filed square steel tube with inner I-shaped CFRP profiles short columns under bi-axial eccentric load decrease with the increase of eccentric ratio, the ultimate bearing capacity of the composite columns increase with the increase of steel ratio, steel yield strength, concrete compressive strength and CFRP distribution rate. The contact pressure between the steel tube and the concrete decreased from the corner zone to the flat zone, and the contact pressure decreased from the mid-height cross section to other sections.

Keywords: I-shaped CFRP; concrete-filed square steel tube; short column; mechanical behavior; finite element analysis.

1. Introduction

Concrete-filled steel tube is a kind of components, which are made in the steel tube and then filling concrete in it. The concrete-filled steel tube components have many advantages, such as high bearing capacity, good plastic, good ductility and good ductility. Because of the advantages, it has been widely used in project. At present, the most common section of the steel tube concrete section in the project is circular, and square [1]. The constraint of the concrete-filled square steel tube is not more uniform than the constraint of the concrete-filled circular steel tube. In the concrete-filled square steel tube, the constraint of the corner zone is bigger than the constraint in the flat zone. However, the concrete-filled square steel tube is much easier to be manufactured and constructed than the concrete-filled circular steel tube, so concrete-filled square steel tube is much more widely

applied in the practical engineering [2]. Up until now, a large number of scholars have studied the concrete-filled steel tube. The scholar Y. Ouyang [3] presented a new finite element model, the model is developed for the analysis by taking into the lateral strain-axial strain relation of the confined concrete covering the full range from the initial elastic stage to the inelastic stage of concrete-filled circular steel tube columns under eccentric load, The finite element model is used to analyze a total of 95 concrete-filled circular steel tube specimens tested by other researchers and the numerical results are compared to the published test results for verification. Tao Zhong and Han Linhai [4] based on the steel and concrete stress-strain model of concrete-filled square steel tubes under axial compression; they calculated and analyzed the load-deformation curve of the concrete filled square steel tubes under biaxial bending or the combination of axial compression and biaxial

bending. After comparing with the experimental results, the simplified formula for calculating the bearing capacity of this type of component is obtained. Tian Hua, Zhang Sumei and others [5-6] based on square, circular steel tubes high strength concrete axial compression short columns, calculated and analyzed the circular steel tubes high strength concrete bi-directional bending members by programming nonlinear numerical calculation program. They considered the influence of two different loading paths, residual stress, slenderness ratio, yield strength of steel, steel ratio and other parameters to the bearing capacity, they obtained the relationship of the three-dimensional bearing capacity and they obtained the simplified formula of the circular steel tube high strength concrete bi-directional bending member.

A large number of scholars add various types of core materials in concrete-filled square steel tube to change the mechanical properties and working performance of concrete-filled square steel tube. Zhao Tongfeng [7] et al. experimental researched 9 square steel tube columns filled with steel reinforced concrete subjected to bi-axial eccentric compression which is with the main parameters; eccentric ratio, eccentric angle and strength of the profile. By comparing with the finite element simulation and the experimental results, they got the conclusion; slenderness ratio, eccentric rate and eccentric angle have great influence on the bearing capacity of the components. Carbon fiber reinforced material (CFRP), as a fiber reinforced composite, has the characteristics of lightweight and high strength. Adding it in civil the engineering can effectively improve the bearing capacity and deformability [8]. Concrete-filed square steel tube with inner I-shaped CFRP profiles is a new component, which is made by putting the CFRP profiles into the concrete-filled square steel tube. At present, there were some research on the axial compression members and eccentric compression members [9-10]. In practical engineering, under the complex loads the columns are often subjected to bi-axial eccentric load, but the research on concrete-filed square steel tube with inner I-shaped CFRP profiles columns under bi-axial eccentric load is still a blank. Therefore, in this paper, we establish 15 short column finite element models by using finite element analysis software ABAQUS to study their mechanical properties.

2. Size design of model

The size of the model section is 150 mm × 150 mm and 450 mm in length. The cross section size of the I-shaped carbon fiber composite profiles is 70 mm × 60 mm × 6 mm. The layout of the components is shown in Fig. 1.
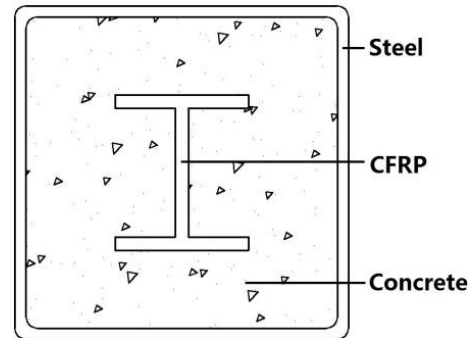

Fig. 1. Component structure diagram.

The model changes with following parameters: eccentric ratio e/R (R=B/2, B is width of cross section, B=150mm, e is the eccentric distance which is between the central point of the component section and the loading place, seeing the details in Fig. 3), yield strength of steel f_y, compressive strength of concrete cube f_{cu}, wall thickness of steel tube t, CFRP distribution rate. The main parameters of the models are referred to in Table 1.

Table 1. Main parameters of the specimens.

Component number	f_y (MPa)	f_{cu} (MPa)	e/R	t (mm)	CFRP
BS-1	345	50	0.133	5	Yes
BS-2	345	50	0.267	5	Yes
BS-3	345	50	0.400	5	Yes
BS-4	345	50	0.533	5	Yes
BS-5	345	50	0.667	5	Yes
BS-6	345	50	0.800	5	Yes
BS-7	390	50	0.267	5	Yes
BS-8	460	50	0.267	5	Yes
BS-9	550	50	0.267	5	Yes
BS-10	345	60	0.267	5	Yes
BS-11	345	70	0.267	5	Yes
BS-12	345	80	0.267	5	Yes
BS-13	345	50	0.267	4	Yes
BS-14	345	50	0.267	6	Yes
BS-15	345	50	0.267	5	No

Notes: B means biaxial, S means square, f_y means the yield strength of steel, f_{cu} means the compressive strength of concrete cube, and t is the wall thickness of steel tube.

3. Constitutive relation model of each material

3.1. Constitutive relation model of steel

Steel tube is made by cold rolled steel. Because of the cold bending hardening of the steel, the steel tube is divided into the corner zone and the flat zone the means of partitioning is shown in Fig. 2. Finite element analyzes the model by using the stress strain relationship model of steel, which was proposed by Abdel-Rahman and Sivakumaran [8-9]. The elastic modulus of steel is 206000 MPa.
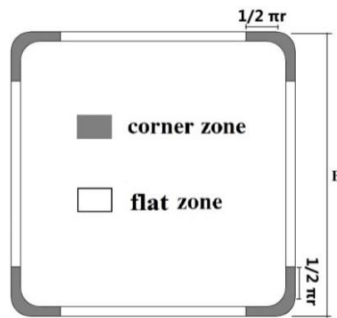

Fig. 2. Flat and corner zone of steel tube.

3.2. Constitutive relation model of concrete

In the initial stage, the constraint on concrete of concrete-filled steel tube is very limited, at this time; the concrete is almost unidirectional force state. As the load continues to increase, the Poisson ratio of the concrete will exceed other two materials, at this time the concrete enters the three-direction force state. Concrete, as a kind of fragile materials, will have split fracture failure, a kind of brittle fracture, under the lower circumferential binding force. The failure forms of concrete are mainly cracked and crushed [10]. In this paper, the plastic damage constitutive model of concrete [11] is used to simulate the finite element method. The elastic modulus of concrete were calculated by $E_c = 4730\sqrt{f_c}$ (MPa) [12]. The Poisson ratio in the elastic phase is 0.2. The tensile zone is controlled by the concrete failure energy criterion. The stress - fission energy relationship and failure stress are used to judge whether the tensile zone destroys [13].

3.3. Constitutive relation model of I-shaped CFRP profiles

4. CFRP I-shaped profiles are molded by pulling, and then the carbon fiber cloth is wrapped on the surface of the profiles. In this paper we use the two dimensional Tsai-Wu failure criterion to distinguish the failure of the I-shaped CFRP profiles. The failure criterion takes into account fiber tensile failure, fiber compression failure, matrix tensile failure, matrix compression failure and shearing failure of matrix fiber to judge whether the profile is destroyed. At the same time, the ABAQUS subprogram USDFLD was secondarily developed to control the damage and failure of the I-shaped CFRP profiles section during the modeling process.

4. Model establishments

Steel tube, concrete and end plates are modeled by C3D8R unit element. CFRP I-shaped composite profiles are modeled by S4R unit element. Hard contact is used to transfer the binding force which is in the vertical direction between the concrete and steel contact surface. Hard contact is used to make it possible to transfer the pressure of the end plates to the concrete surface. The Coulomb friction model which is provided by the ABAQUS finite element analysis software is used to transfer the tangential direction of the concrete surface and the steel surface, the Coulomb friction coefficient is 0.6. Tie binding constraints is used between steel tube and end plates and between CFRP profiles and concrete, shell-solid. Coupling constraints is used between I-shaped CFRP profiles and end plates. Loading end boundary condition is $U_1 = U_2 = UR_3 = 0$, fix end boundary condition is $U_1 = U_2 = U_3 = UR_3 = 0$, using the condition simulate the concrete-filled square steel tubes under bi-axial eccentric load. The process of establishing the finite element analysis model is shown in Fig. 3.
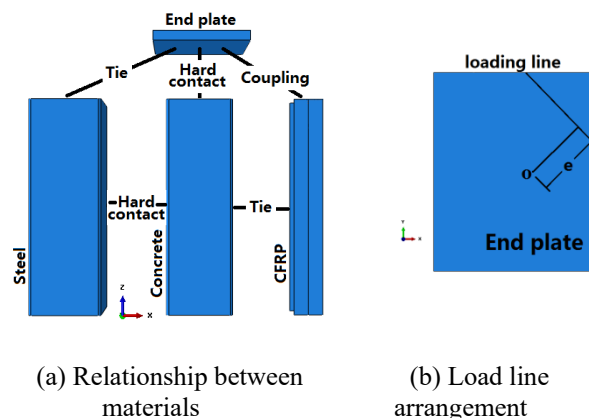

| (a) Relationship between materials | (b) Load line arrangement |

Fig. 3. Finite element analysis model.

5. Analysis of the whole process of the N-μm curve

Select the BS-2 component as a typical component. By the finite element analyzing, the N-μ_m curve is obtained (μ_m is the deflection of the middle section) which is shown in Fig. 4. The N-μ_m curve can be divided into four stages; O-A stage, elastic stage, concrete, steel and I-shaped CFRP profiles are separately subjected to force. At A point, the maximum longitudinal stress reaches the limit of proportionality in the section of steel tubes. A-B stage, elastic plastic stage, with the vertical load gradual increasing, concrete will product transverse plastic deformation, but because of the existence of the steel tubes, it will restrict the development of the concrete transverse deformation. The longitudinal stress of the concrete in the corner is greater than the ultimate compressive strength. Before the point B, the longitudinal strain of the concrete is beyond the concrete ultimate compressive strain, at this time the concrete crushed. When the B point is reached, most of the steel tube zone reached the plastic stage. B-C stage, downward stage, when the load reaches the peak load, the longitudinal fiber of the I-shaped CFRP profiles in the section profile drawing zone flange is broken, and then the load will drop significantly. C-D stage, gentle stage, at this stage, the load descends slowly but the lateral deflection of the component develops rapidly.
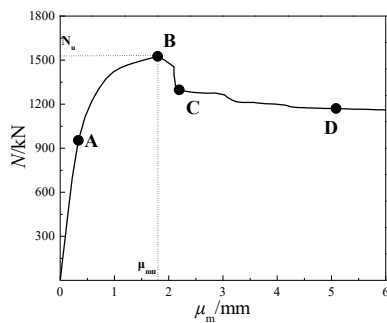

Fig. 4. The N-μ_m curve.

Fig. 5 is longitudinal stress isoclines map of the core concrete in the BS-2 component at the three characteristic points A, B and C. At A point, from the corner of the compression area to the corner of the tension zone the longitudinal stress of the core concrete section is zonally distributed. At this time, the area of the compressed zone is larger than the area of the

drawing zone. The maximum stress in the compression zone is much greater than the maximum stress in the tension zone. The maximum compressive stress is 11.43 times of the maximum tensile stress. The stress in the corner of the compression zone reaches $1.0 \cdot f_c$. At B point, the longitudinal compression stress of the concrete in the corner area reaches $1.28 \cdot f_c$. The concrete near the end of the compressed flanking edge of the profile is only $0.15 \cdot f_c$. The longitudinal compression stress of the concrete between the junction of the flanking and the flat reaches f_c and $0.79 \cdot f_c$. At C point, the longitudinal compression stress of concrete in the corner zone reaches $1.29 \cdot f_c$, $1.39 \cdot f_c$ and $1.40 \cdot f_c$ respectively. The longitudinal compression stress of concrete at the flat zone of steel reaches $1.10 \cdot f_c$. It can be obtained that the constraint between the steel and the concrete is mainly concentrated in the corner zone.
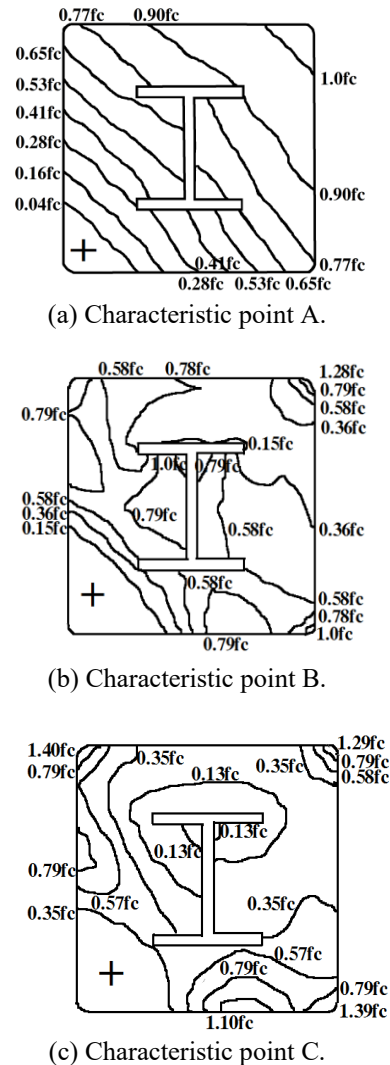

(a) Characteristic point A.

(b) Characteristic point B.

(c) Characteristic point C.

Fig. 5. Longitudinal stress isoclines map of the core concrete in the middle section of the three characteristic points.

Fig. 6 is the longitudinal stress distribution of the I-shaped CFRP profile at the three characteristic points A, B, and C of the BS-2 component. At the initial stage of loading, the I-shaped CFRP profile full section is compressed. The longitudinal stress of the flange near the compression zone is obviously greater than the longitudinal stress on the other side of the flange. The longitudinal stress of the flanges near the concrete compression zone at A point is 2.7 times of the longitudinal stress on the other side. At B point, it is 4.9 times the other side. Between the B point and the C point, the brittle failure occurs outside the flange of the I-shaped CFRP profile section near the compression zone, and then it goes out of work and gradually develops to the flat zone as the load increases. At C point, the section of the I-shaped CFRP profile which is near the compression side drop out working.
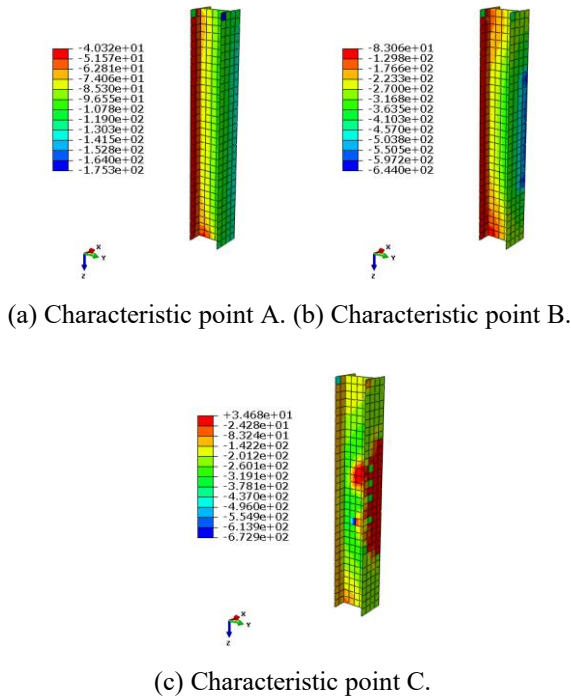
corner zone near the neutral axis reached the yield stage.

(a) Characteristic point A.

(b) Characteristic point B.

(c) Characteristic point C.
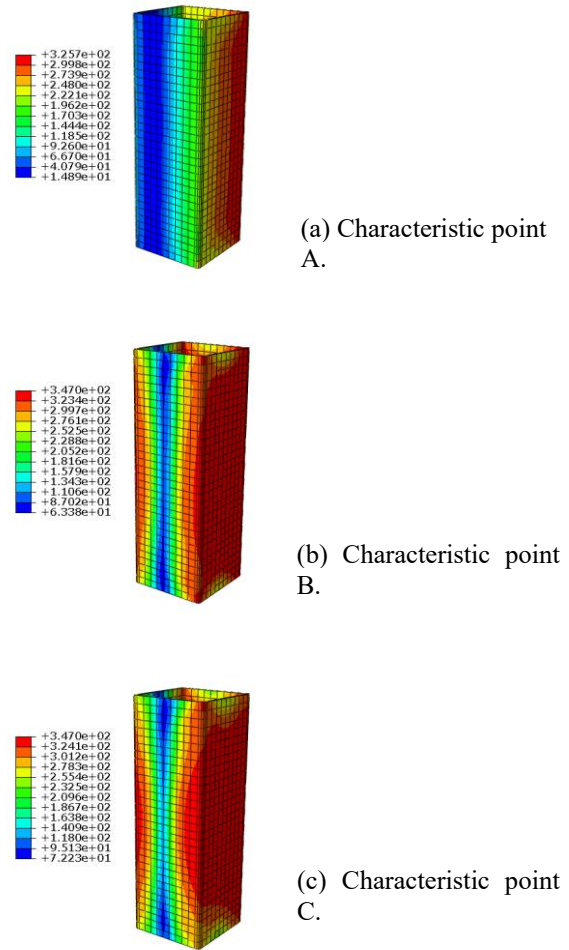
Fig. 7. Von Mises stress contour plots of the steel tube at three characteristic points.

(a) Characteristic point A. (b) Characteristic point B.

(c) Characteristic point C.

Fig. 6. Longitudinal stress distribution map of CFRP profile corresponding to three characteristic points.

Fig. 7 is the Mises stress contour plots of the steel tube at characteristic points A, B, C, of the component BS-2. In the whole process of loading, the stress of Mises in the corner of the steel tubes reached to the yield state firstly, and then quickly spreads to the both sides of the flat zone. At B point, the limit load point, the most zone of the steel tube reached the yield state, yield zone diffuse speed slowly down, the steel

6. Parameter analyses

6.1. Eccentricity ratio e/R

Fig. 8 shows the effect of eccentric ratio on the N-μ_m curve of model BS-1 to model BS-6 (eccentric ratio=0.133~0.800).
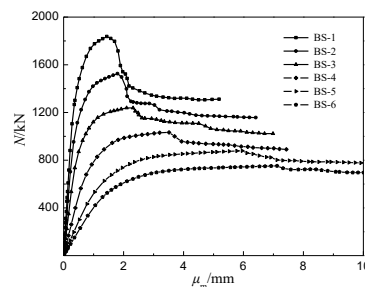

Fig. 8. Effect of eccentric ratio on the N-μ_m curve.

The results show that the ultimate bearing capacity of the six models reduce by 17.80%, 18.31%, 16.69%, 15.38%, 14.40%, with the eccentric ratio of the six models increases 0.133, respectively. At the same time, we can see that The ductility of the components increase with the increase of eccentric ratio, and the ductility coefficient increases from 2.51 to 3.66 (ductility factor is the ratio of the lateral displacement when the component reach ultimate bearing capacity, to the lateral displacement of the member, when the steel tube is yielding). It can be seen that the eccentric ratio has a significant effect on the ultimate bearing capacity and ductility of the components. Fig. 9 shows longitudinal stress isoclines of core concrete of model BS-1, model BS-3 and model BS-5 at the bearing capacity of components. It can be seen that, with the increment of eccentricity, the area of tension zone of model cross section increases gradually, when the model reaches the bearing capacity. When the eccentricity ratio is small (such as eccentricity ratio=0.133, BS-1 component), the whole cross-section of the core concrete is under pressure state.
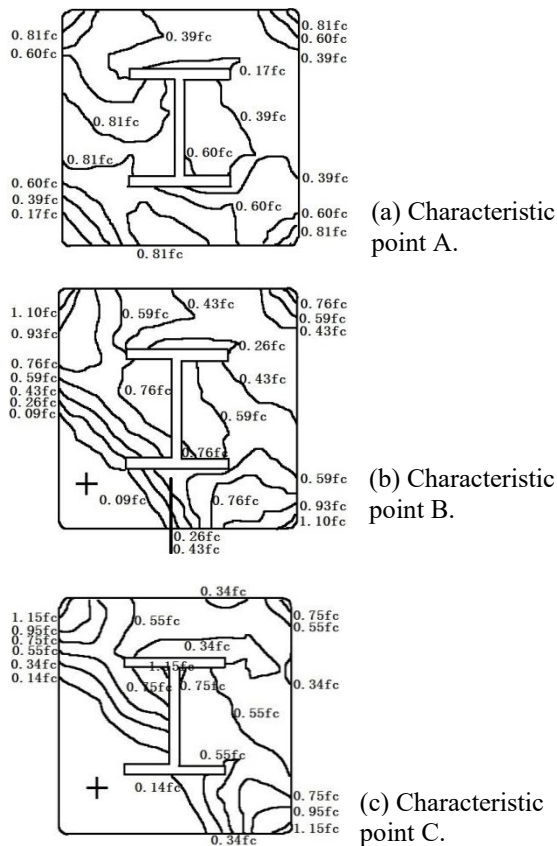

(a) Characteristic point A.

(b) Characteristic point B.

(c) Characteristic point C.

Fig. 9. Effect of eccentricity on longitudinal stress distribution of core concrete in middle section.

6.2. Steel ratio

Fig. 10 is the effect of different steel ratio on the N-μ_m curve of BS-2, BS-13 and BS-14 components. The calculation results show that, the corresponding ultimate bearing capacity increases by 12.30% and 10% respectively with the steel ratio increases by 3.2%, 3.3%. The reason is that, with the thickness of steel tube increases, the restraint ability of steel tube to the core concrete and the CFRP I-shaped profile increase. Nevertheless, the increment of steel tube thickness is little effect on initial stiffness of the N-μ_m curve.
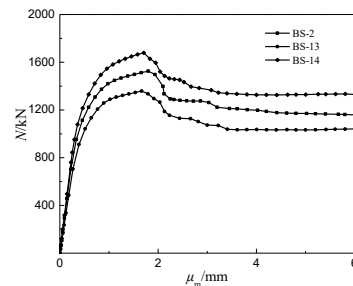

Fig. 10. Effect of different steel ratio on the N-μ_m curve.

6.3. Yield strength of steel f_y

Fig. 11 is the effect of yield strength of steel f_y on the N-μ_m curve of 4 components, in the elastic section, the N-μ_m curve of different components almost coincide, but the sequence of entering the elastic-plastic section is different. While the components go into the elastic plastic stage, the greater the yield strength of the steel is, the greater the load and the deflection of the middle section is, which is corresponding to the characteristic the point A. With the yield strength of steel increased by 13.00%, 17.90%, 19.60%, the ultimate bearing capacity increased by 6.70%, 9.14%, 10.52%, respectively. Therefore, it can be seen that the increment of yield strength of steel has little effect on ultimate bearing capacity.

6.4. Compressive strength of concrete f_{cu}

Fig. 12 shows the effect of compressive strength of concrete f_{cu} on the N-μ_m curve of 4 components. Concrete compressive strength is from 50MPa to 80MPa, the ultimate bearing capacity only increased by 15.49%. The N-μ_m curves are almost coinciding at the elastic stage. It can be seen that increasing the compressive strength of concrete has little effect on the elastic stage and ultimate bearing capacity of the short

columns. With the improvement of the concrete compressive strength, the lateral deflection decreases gradually, when the columns reach the ultimate bearing capacity. With the improvement of the concrete compressive strength, a situation of two peaks in the specimens is appearing. As the concrete compressive strength is improving, the situation of two peaks is more and more obvious, and the ultimate bearing capacity moves to the peak deflection, which has small middle section deflection. At this time, the short columns have less deformation when the columns are damaged. It will have more abrupt destruction.
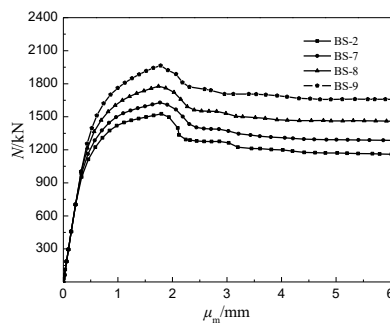

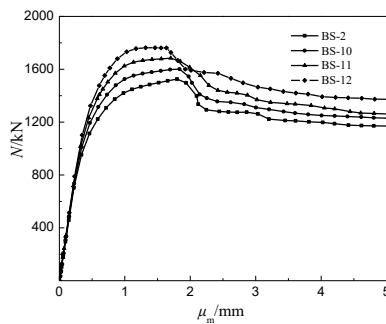*Fig. 11.* The effect of yield strength of steel f_y on the N-μ_m curve.

Fig. 12. Effect of compressive strength of concrete fcu on the N-μ_m curve.

6.5. Configuration of CFRP shaped profile

Fig. 13 shows the effect of configuring I-shaped CFRP profile on the N-μ_m curve. The ultimate bearing capacity of the concrete-filed square steel tube with inner I-shaped CFRP profile short column under bi-axial eccentric load is 19.54% higher than the concrete-filled square steel tube short column without the configuration of the I-shaped CFRP profile. At the same time, the lateral deflection corresponding to the ultimate bearing capacity of

the concrete-filed square steel tube with inner I-shaped CFRP profile short column with inner I-shaped CFRP profile is significantly improved. The descending segment of the N-μ_m curve is steeper, and there is more abrupt destruction.
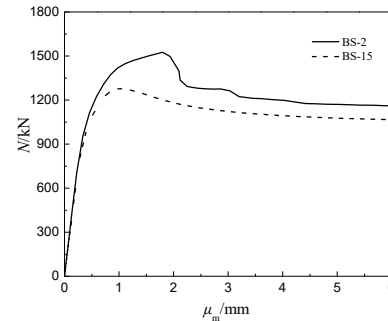

Fig. 13. Effect of configuring CFRP I-shaped profile on the N-μ_m curve.

7. Conclusions

1. The ultimate bearing capacity and deformability of concrete filled steel square tube can be effectively improved after configuring CFRP shaped profile, and the N-μ_m curve can be divided into four stages: elastic stage, elastic plastic stage, downward stage and gentle stage.

2. The binding effect of steel to concrete is mainly concentrated in the corner of the compression zone. The effect of CFRP shaped profile to concrete is mainly concentrated on the boundary between the flange and the flat. The steel in the flat zone and the steel in the corner of the tension zone cannot restrict to the concrete very well.

3. The eccentric ratio has the greatest influence on the N-μ_m curves of the concrete-filed square steel tube with inner I-shaped CFRP profile short columns under bi-axial eccentric load short columns, the steel ratio and the yield strength of steel has less influence on the N-μ_m curves, The compressive strength of concrete has the least influence on the N-μ_m curves.

References

[1] Han LH. Concrete-filled steel tube structures-Theory and Practice (in Chinese). 3rd ed. Beijing: Science Press; 2016.

[2] Cai J, Pan J, Shan Q. Failure mechanism of full-size concrete-filled steel circle and square tubes under uniaxial compression. Science China Technological Science 2015; 58: 1638-1647.

[3] Ouyang Y, Kwan AKH, Lo SH, Ho JCM. Finite element analysis of concrete-filled steel tube (CFST) columns with circular sections under eccentric load. Engineering Structures 2017; 148: 387-398.

[4] Zhong T, Han LH. Theoretical analysis and simplified calculation of concrete-filled square steel tubular member subjected to axial compression and biaxial bending (in Chinese). Steel Construction 2000; 15(1): 42-46.

[5] Tian H, Zhang S, Guo L. Cross-sectional strength of high-strength concrete-filled RHS steel tubes subjected to axial compression and bi-axial bending moment (in Chinese). Journal of Harbin Institute of Technology 2007; 39(10): 1520-1528.

[6] Tian H, Zhang S, Guo L. Behavior of high-strength concrete-filled RHS steel tubular members subjected to axial compression combined with bi-axial bending (in Chinese). Journal of Harbin Institute of Technology 2007; 39(12): 1854-1858.

[7] Zhao T, Ouyang W, Li D. Experiment research and finite element analysis of square steel tube columns filled with steel reinforced concrete subjected to bi-axial eccentric compression (in Chinese). Building Structure 2011; 41(8): 87-91.

[8] Wo D. Encyclopedia of Composites (in Chinese). Beijing: Chemical Industry Press; 2002.

[9] Zhou B. Study on mechanical behavior of concrete-filled square steel short column with inner CFRP I-shaped profiles under axial compression (in Chinese). Shen Yang: Shenyang Jianzhu University; 2014.

[10] Sun X, Li G, Yang Z, Liu X. Finite element analysis of mechanical behavior of concrete-filled square steel tube middle-long columns with inner I-shaped CFRP profiles under eccentric loading (in Chinese). Industrial Construction 2017; 47(3): 157-162.

[11] Karren KW. Corner properties of cold-formed steel shapes. Journal of the Structural Division 1967; 93(2): 401-432.

[12] Abdel-Rahman N, Sivakumaran KS. Material properties models for analysis of cold-formed steel members. Journal of Structural Engineering 1997; 123(9): 1135-1143.

[13] Yao G, Huang Y, Song B, Tan W. Analysis for static behaviour of steel and concrete composite members with plastic-damage model (in Chinese). Progress in Steel Building Structures 2009; 11(3): 12-18.

[14] Liu W. Research on mechanism of concrete-filled steel tubes subjected to local compression (in Chinese). Fuzhou University; 2005.

[15] ACI 318-05. Building code requirements for structural concrete and commentary. Farmington Hills (MI), American Concrete Institute, Detroit: USA; 2005.

[16] Shen J, Wang C, Jiang J. Finite element method of reinforced concrete and limit analysis of plates and shells (in Chinese). Beijing: Tsinghua University Press; 1993.